Lattice distortion in Cu-based dilute alloys: A first-principles study by the KKR Green-function method

N. Papanikolaou, R. Zeller, and P. H. Dederichs
Institut für Festkörperforschung, Forschungszentrum Jülich D-52425 Jülich, Germany

N. Stefanou
University of Athens, Section of Solid State Physics, Panepistimioupolis GR-15784 Athens, Greece
(Received 13 September 1996)

The full-potential Korringa-Kohn-Rostoker Green function method is extended to treat the lattice distortion in the vicinity of a point defect. The method is applied to predict the atomic positions in the neighborhood of *d* and *sp* substitutional impurities in Cu. Both the total energy and the Hellmann-Feynman force are used for the calculation of the ground-state configuration, while the semicore states of the impurities are treated as valence states. Our results for the atomic displacements are in very good agreement with the experimental data from extended x-ray-absorption fine-structure and lattice-parameter measurements. [S0163-1829(97)07907-1]

I. INTRODUCTION

The presence of a point defect in a crystal, such as a vacancy or an impurity atom, generally causes a displacement of the neighboring host atoms from their ideal lattice positions. For alloys, such a lattice distortion changes the lattice constant and this change can be measured by x-ray diffraction. However, this information is not sufficient to estimate the interatomic distances because, generally, the distortion is different in magnitude for different atomic shells around the defect. More detailed information can be obtained by extended x-ray-absorption fine-structure (EXAFS) experiments, in which the absorption spectrum of the emitted photoelectrons from the excited atom, as being modified by the backscattering from the surrounding atoms, is measured. A systematic study of the lattice relaxation around substitutional impurities has been reported by Scheuer and Lengeler,[1] who measured interatomic distances, coordination numbers, and Debye-Waller factors using EXAFS. Nevertheless, even EXAFS measurements can give reliable information only for the displacement of the first nearest neighbors (NN's) and, moreover, the results depend to some extent on the model used to interpret the experimental data. Diffuse x-ray or neutron scattering can give more complete information on local geometries, albeit for substitutional impurities very few experiments have been performed so far. For many defect properties, e.g., solution or interaction energies, residual resistivities, and NMR quantities, the importance of the lattice distortion is not clear and a detailed understanding is still far from being complete.

From the theoretical point of view the treatment of structural relaxation due to defects in crystals is a difficult task. In the past this problem has been mostly dealt with on a phenomenological basis, e.g., by applying models of lattice statics or continuum theory.[2] Various semiempirical methods have been also employed, especially for defects in semiconductors.[3] A reliable microscopic description of lattice relaxation effects based on first-principles electronic-structure calculations requires very accurate total energies or forces and has mostly been attempted so far for simple metals and semiconductors on the basis of pseudopotential treatments. The difficulty arises mainly from the fact that energy differences due to local atomic displacements are quite small, of the order of 0.1 eV, compared with, e.g., the cohesive energy of the solid. The pseudopotential supercell approach has been used to describe structural distortion in simple-metal[4] and semiconductor[5–7] systems. Lattice relaxation effects around defects in semiconductors have also been treated by the pseudopotential Green-function method.[8–10] Within the cluster approach a large finite cluster of atoms is used to simulate the macroscopic crystal. Structural distortions have been studied by this method for defects in metals,[11] semiconductors,[12] and ionic systems.[13]

Nowadays self-consistent, all-electron calculations of the electronic structure of solids can be carried out by employing the first-principles computational formalisms developed in recent years. Among these formalisms, the full-potential Korringa-Kohn-Rostoker (KKR) Green-function method offers an elegant and efficient framework for the treatment of the defect problem. Our aim in the present paper is to present an extension of this method in order to treat the lattice distortion around point defects in crystals. The method is applied to study the local geometry in the neighborhood of *d* and *sp* impurities in bulk Cu. In this respect we have performed both total-energy and force calculations by considering the perturbation of several atomic shells around the impurity atom, while the chemical environment of the host is described by the Green function. We first give a short description of our method and present the formalism for the force calculation that is based on the Hellmann-Feynman (HF) theorem. Section III deals with some technical aspects of the computation. In Sec. IV we discuss our results for interatomic distances, volume changes, relaxation energies, and local magnetism for Cu-based dilute alloys and compare with experimental data from EXAFS and lattice-parameter measurements. Section V summarizes the main results of the paper.

II. THEORETICAL METHOD

A. Full-potential multiple-scattering theory for a crystal with a moderate lattice distortion

Within the framework of the KKR multiple-scattering theory a crystalline solid is divided into nonoverlapping space-filling cells around each atomic cite $\mathbf{R}_n$. The effective one-electron potential is written as a collection of individual potentials $V^n(\mathbf{r})$, where the position vector $\mathbf{r}$ is restricted within cell n. Using a site-centered expansion, the crystal Green function can be written in the form[14]

$$G(\mathbf{r}+\mathbf{R}_n,\mathbf{r}'+\mathbf{R}_{n'};E)=\delta_{nn'}G_s^n(\mathbf{r}+\mathbf{R}_n,\mathbf{r}'+\mathbf{R}_{n'};E)+\sum_{L,L'}R_L^n(\mathbf{r};E)G_{LL'}^{nn'}(E)R_{L'}^{n'}(\mathbf{r}';E), \tag{1}$$

where G_s^n is the Green function for a single scattering potential in cell n in an otherwise free space. Multiple-scattering contributions are contained in the second term through the so-called structural Green function $G_{LL'}^{nn'}(E)$. The index L denotes the angular momentum quantum numbers (l,m) and $R_L^n(\mathbf{r};E)$ are regular partial-wave solutions of the Schrödinger equation for the potential $V^n(\mathbf{r})$ and energy E.

The electronic structure of a crystal with a localized perturbation, induced by the presence of a point defect for instance, can be obtained in two steps. We first calculate the ideal host Green function G^0 following a band-structure calculation[15,16] and obtain the host structural Green function $G_{LL'}^{0nn'}$ from Eq. (1). The Green function of the defect system can be then calculated in a second step from expansion (1), with the structural Green function given by the solution of the algebraic Dyson equation[14]

$$G_{LL'}^{nn'}(E)=G_{LL'}^{0nn'}(E)+\sum_{n'',L'',L'''}G_{LL''}^{0nn''}(E)\Delta t_{L''L'''}^{n''}(E)G_{L'''L'}^{n''n'}(E). \tag{2}$$

The summations in Eq. (2) extend only over those cells and angular momenta where the difference $\Delta t_{LL'}^n(E)$ between the t matrices of the defect and the host system is significant. Equation (2) can be abbreviated in matrix form: $\mathcal{G}=\mathcal{G}^0+\mathcal{G}^0\Delta t\mathcal{G}$.

For general potentials that include nonspherical contributions, we expand wave functions and potentials in real spherical harmonics

$$R_L^n(\mathbf{r};E)=\sum_{L'}R_{L'L}^n(r;E)Y_{L'}(\hat{\mathbf{r}}), \tag{3}$$

$$V^n(\mathbf{r})=\sum_L V_L^n(r)Y_L(\hat{\mathbf{r}}). \tag{4}$$

The nonspherical components of the potential couple the angular momentum channels and one is faced with the problem of a system of coupled radial equations. We solve the problem as follows. We first calculate the wave function for the spherical part of the potential and then treat the nonspherical contribution by iterative solution of a Lippmann-Schwinger-type integral equation. Since the anisotropic components are generally small, the iterations converge fast and the second Born approximation is usually sufficient to obtain well-converged total energies and forces.[16–18] Moreover, close to the nucleus the potential is almost spherical, so the nonspherical contributions are only calculated for radii larger than a cutoff radius S_0. For the total-energy calculation it is sufficient to choose S_0 to be about half the muffin-tin radius.[16] However, the force calculation requires more accurate charge densities and thus we have used an $S_0=0.15a_B$, where a_B is the Bohr radius, which ensures well-converged results for the forces.

The electron density in cell n can be calculated by integrating the site-diagonal elements of the Green function over all occupied states, up to the Fermi energy E_F,

$$n^n(\mathbf{r})=-\frac{1}{\pi}\mathrm{Im}\int_{-\infty}^{E_F}dEG(\mathbf{r}+\mathbf{R}_n,\mathbf{r}+\mathbf{R}_n;E). \tag{5}$$

Taking advantage of the analytical properties of the Green function, the valence density can be obtained from Eq. (5) by replacing the integral on the real energy axis with a contour integral in the complex energy plane that starts below the valence band and ends at the Fermi energy. In this way a much smaller number of energy points can be used for the integration since the Green function is less structured as we move away from the real axis.[19]

Let us now suppose that we introduce a distortion in the crystal, shifting a number of atoms by $\mathbf{s}_n$ from their ideal lattice sites. The structural Green-function matrix of the ideal host can be expanded around the shifted atomic positions, with the help of the transformation[20,21]

$$\tilde{\mathcal{G}}^0=\mathcal{U}\mathcal{G}^0\mathcal{U}^{-1}. \tag{6}$$

The transformation matrix $\mathcal{U}$ is local in the site index and is given by

$$U_{LL'}(\mathbf{s}_n;E)=4\pi\sum_{L''}i^{l+l''-l'}C_{LL'L''}j_{l''}(s_n\sqrt{2mE}/\hbar)Y_{L''}(\hat{\mathbf{s}}_n), \tag{7}$$

where j_l are spherical Bessel functions and $C_{LL'L''}=\int d\hat{\mathbf{r}}Y_L(\hat{\mathbf{r}})Y_{L'}(\hat{\mathbf{r}})Y_{L''}(\hat{\mathbf{r}})$ are the Gaunt coefficients. The following properties can be directly derived from Eq. (7):

$$U_{LL'}(\mathbf{s}_n;E)=(-1)^{l+l'}U_{L'L}(\mathbf{s}_n;E), \tag{8}$$

$$[U^{-1}(\mathbf{s}_n;E)]_{LL'}=U_{LL'}(-\mathbf{s}_n;E)=U_{L'L}(\mathbf{s}_n;E). \tag{9}$$

For lattice distortions, the defect structural Green function $\mathcal{G}$, which is expanded in the shifted coordinate system, can be related to the host structural Green function by the Dyson equation

$$\mathcal{G}=\tilde{\mathcal{G}}^0+\tilde{\mathcal{G}}^0(t-\tilde{t}^0)\mathcal{G}, \tag{10}$$

where $\tilde{t}^0=\mathcal{U}t^0\mathcal{U}^{-1}$ is the ideal host t matrix in the expansion around the shifted sites and t is the defect t matrix. We have used a tilde to denote quantities that are obtained using a coordinate system transformation. In Eq. (10) all quantities

are expanded around the shifted centers. Alternatively, one can transform the Dyson equation (10) to the unshifted coordinate system

$$\underset{\sim}{\mathcal{G}}=\mathcal{G}^0+\mathcal{G}^0(\boldsymbol{t}-t^0)\underset{\sim}{\mathcal{G}}, \tag{11}$$

with

$$\boldsymbol{t}=\mathcal{U}^{-1}t\mathcal{U}, \quad \underset{\sim}{\mathcal{G}}=\mathcal{U}^{-1}\mathcal{G}\mathcal{U}, \tag{12}$$

and, after solving Eq. (11), transform the defect Green function back to the shifted coordinate system by

$$\mathcal{G}=\mathcal{U}\underset{\sim}{\mathcal{G}}\mathcal{U}^{-1}. \tag{13}$$

Both schemes [Eqs. (10) and (11)–(13)] are equivalent; however, the latter is more convenient since it reduces the additional computational effort when treating structural changes. This can be easily understood since only the site-diagonal elements $G^{nn}_{LL'}(E)$ of the defect structural Green function are needed for the calculation of the charge density and, therefore, only these have to be transformed to the shifted system.

A problem occurring in the transformation of the Green function or the t matrix is the angular momentum convergence. However, for small shifts, to first order in the displacement, the only nonvanishing off-diagonal elements of the transformation matrix (7) are those with $|l-l'|=1$.[21] Therefore, for moderate lattice distortions, accurate calculations up to $l_{\max}$ can be done if angular momentum components up to $l_{\max}+1$ are included. The full-potential KKR Green-function method has been found to give accurate, well-converged total energies[16] and forces[22] using a cutoff at $l_{\max}=3$. Therefore, in the present calculation we use $l_{\max}=4$ in order to obtain reliable results.

In solving Schrödinger and Poisson equations the space is divided into space-filling, nonoverlapping cells, described by the shape functions $\Theta^n(\mathbf{r})$, which equal 1 inside cell n and vanish outside. The shape functions are expanded in real spherical harmonics

$$\Theta^n(\mathbf{r})=\sum_L \Theta^n_L(r)Y_L(\hat{\mathbf{r}}). \tag{14}$$

The expansion coefficients

$$\Theta^n_L(r)=\int d\hat{\mathbf{r}}\Theta^n(\mathbf{r})Y_L(\hat{\mathbf{r}}) \tag{15}$$

are calculated with the algorithm of Stefanou *et al.*[23] following a semianalytical approach that can be used for any arbitrary Voronoi polyhedron. For a distorted lattice one can either make a Wigner-Seitz (WS) construction in the distorted geometry or keep the same space division as in the undistorted lattice and just calculate the shape functions expanded around the shifted centers. The latter procedure is preferable when the displacements are small (of the order of a few percent) and is the one we have used in the present work. However, for larger displacements the former procedure seems to be a better choice because it optimizes the angular momentum convergence of the wave functions.

A problem connected with the use of the shape functions is that the expansion coefficients $\Theta^n_L(r)$ have kinks (i.e., discontinuities of the first derivative) for radii that correspond to the distance of a face, an edge, or a vertex of the polyhedron from the center.[23] Since a shape function truncates the potential within a WS cell, these discontinuities are also present in the first derivative of the potential. For a fcc WS cell, for example, the shape function introduces three kinks. To avoid inaccuracies in the numerical integration of Schrödinger equation caused by the kinks, we can restart the integration of the Schrödinger equation at each kink. Although this procedure is the one that we use in the present work, it is not very efficient for nonsymmetric polyhedra because the number of kinks increases and one typically has to deal with 20 or 30 kinks. For this purpose it is preferable to replace the shape functions (14) by broadened functions $\overline{\Theta^n}(\mathbf{r})$ with the virtue of the Fermi-Dirac distribution. Since the derivative of the step function is a δ function, the smeared shape functions can be found from

$$\overline{\Theta^n_L}(r)=\int dx\Theta^n_L(r+x)\,\overline{\delta}(x), \tag{16}$$

where

$$\overline{\delta}(x)=\frac{1}{\tau}\frac{e^{-x/\tau}}{(e^{-x/\tau}+1)^2} \tag{17}$$

is the derivative of a Fermi-Dirac-like function. By optimizing the ''temperature'' parameter τ we can render $\overline{\Theta^n_L}(r)$ smooth enough in order to ensure an accurate evaluation of total energies and forces.

B. Total energy

The calculation of the total energy is more complicated in a defect system than in a periodic crystal. The main reason is that Friedel screening rule cannot be satisfied exactly if one limits the perturbation to a finite region of space surrounding the defect and, moreover, truncates the angular momentum expansions. This means that the total number of electrons of the system N cannot be conserved so that the extremal properties of the Kohn-Sham energy functional are lost. This problem can be overcome by introducing a generalized energy functional[18]

$$\widetilde{E}\{n(\mathbf{r})\}=E\{n(\mathbf{r})\}-E_F\left(\int d^3r n(\mathbf{r})-N\right), \tag{18}$$

where $E\{n(\mathbf{r})\}$ is the Kohn-Sham energy functional.[24] Here and in what follows, unless otherwise stated, $\mathbf{r}$ is used to denote any point in the crystal, no longer being restricted within an atomic cell. The generalized functional defined by Eq. (18) retains its extremal properties even for non-particle-conserving variations of the charge density. The total energy is separated into single-particle and double-counting contributions. The single-particle energy is calculated using Lloyd's formula, adapted for complex energies[18] and full potentials,[16] which sums up the energy contributions from the charge perturbation in all space. In this way the change of the total energy due to the defect is well converged by including the perturbation of only a few atomic shells around the impurity atom.

C. Hellmann-Feynman forces and the core polarization problem

The HF theorem[25] offers an attractive way to calculate forces, since a single self-consistent calculation is sufficient to obtain the forces on all atoms. However, this is also a rather difficult scheme, because the correct charge density is required. As stated by the HF theorem, the force on a nucleus with nuclear charge Z_n at position $\mathbf{R}_n$ is given by the electric field $\mathbf{E}(\mathbf{R}_n)$ due to all other nuclei and all electrons

$$\mathbf{F}^n = Z_n \mathbf{E}(\mathbf{R}_n) = -Z_n \left\{ \sum_{n' \neq n} \left(\partial_{\mathbf{R}_n} \frac{1}{|\mathbf{R}_n - \mathbf{R}_{n'}|} \right) Z_{n'} - \int d^3r' \left(\partial_{\mathbf{R}_n} \frac{1}{|\mathbf{r}' - \mathbf{R}_n|} \right) \rho(\mathbf{r}') \right\}, \tag{19}$$

where the integration extends over the whole crystal and $\rho(\mathbf{r}) = |e| n(\mathbf{r})$. While Eq. (19) is exact, its application in realistic calculations is problematic since highly accurate charge densities are needed. The reason for this is that in deriving $\mathbf{F}^n$ as the gradient of the total energy with respect to the nuclear coordinate $\mathbf{R}_n$, one uses the Euler-Langrange equations, which are valid only for the correct charge density. As a consequence, one is no longer protected by the extremal properties of the total energy and first-order errors in the charge density lead to first-order errors in the force. The HF force given by Eq. (19) is directly proportional to the bare nuclear charge Z_n, instead of an effective ionic charge as one would intuitively expect. Thus the question arises whether one can derive an ''ionic'' force formula equivalent to the nuclear one (19). In such a treatment the core electrons would screen the nuclear charge, so that effectively the force on the ion, i.e., on the nucleus and on the core electrons, would have to be calculated. Such an ionic formula for the force has been derived by Harris *et al.*[26] In this treatment one starts with the total energy in the frozen-core approximation and then takes the derivative with respect to $\mathbf{R}_n$ by using the Euler-Langrange equations only for the valence electrons and not for the core electrons. The force formula derived in this way is still extremal with respect to variations of the core charge density, so that reliable forces can be calculated if the valence density is accurate. In the following we will give a somewhat more general derivation of the ionic HF formula, which shows more clearly the equivalence of the nuclear and the ionic HF formula.

The charge density of the core electrons in a solid can be in a very good approximation considered to be spherically symmetric. However when one calculates the HF force by (19), this approximation is not sufficient for the on-site electrons, since the core density is weighted by a large factor $1/|\mathbf{r} - \mathbf{R}_n|^2$ and a spherical approximation for the core gives no contribution at all. Therefore, we write the total core charge density as

$$\rho_c(\mathbf{r}) = \rho_c^{0n}(|\mathbf{r} - \mathbf{R}_n|) + \Delta\rho_c^n(\mathbf{r} - \mathbf{R}_n) + \sum_{n' \neq n} \rho_c^{0n'}(|\mathbf{r} - \mathbf{R}_{n'}|), \tag{20}$$

where $\Delta\rho_c^n(\mathbf{r} - \mathbf{R}_n)$ represents the anisotropic polarization of the core states in cell n due to the anisotropic part of the potential in this cell, which is induced by the valence charge density. The anisotropy of the core charge densities of the other nuclei are here neglected since the spherical approximation gives already the dominant contribution.

Within first-order perturbation theory the nonspherical part of the core charge density is related to the nonspherical part of the effective potential in cell n, $\Delta V^n(\mathbf{r} - \mathbf{R}_n)$, by the equation

$$\Delta\rho_c^n(\mathbf{r} - \mathbf{R}_n) = \int d^3r' \chi^n(\mathbf{r} - \mathbf{R}_n, \mathbf{r}' - \mathbf{R}_n) \Delta V^n(\mathbf{r}' - \mathbf{R}_n), \tag{21}$$

where χ^n is the core susceptibility calculated with core orbitals that are eigenfunctions of the spherically symmetric component of the effective potential. Inserting Eqs. (21) and Eq. (20), into (19) we obtain

$$\mathbf{F}^n = -Z_n \left\{ \sum_{n' \neq n} \left(\partial_{\mathbf{R}_n} \frac{1}{|\mathbf{R}_n - \mathbf{R}_{n'}|} \right) Z_{n'} - \int d^3r' \left(\partial_{\mathbf{R}_n} \frac{1}{|\mathbf{r}' - \mathbf{R}_n|} \right) \tilde{\rho}(\mathbf{r}') \right\} + Z_n \int d^3r' d^3r'' \left(\partial_{\mathbf{R}_n} \frac{1}{|\mathbf{r}' - \mathbf{R}_n|} \right) \times \chi^n(\mathbf{r}' - \mathbf{R}_n, \mathbf{r}'' - \mathbf{R}_n) \Delta V^n(\mathbf{r}'' - \mathbf{R}_n), \tag{22}$$

where $\tilde{\rho}(\mathbf{r})$ is the sum of the valence density and the spherically symmetric core density. The second term in Eq. (22), which we denote by $\mathbf{F}^n_{\mathrm{pol}}$, is the force on the nucleus due to the anisotropic polarization of the local core wave functions. Thus calculating the force on the nucleus requires an anisotropic treatment of the local core electrons, at least in first-order perturbation theory. This is the major difficulty in working with the nuclear force formula (19). The symmetry of the core susceptibility $\chi^n(\mathbf{r} - \mathbf{R}_n, \mathbf{r}' - \mathbf{R}_n) = \chi^n(\mathbf{r}' - \mathbf{R}_n, \mathbf{r} - \mathbf{R}_n)$ allows a different interpretation of the polarization term in Eq. (22). By exchanging the order of the r' and r'' integration we obtain

$$\mathbf{F}^n_{\mathrm{pol}} = \int d^3r'' \Delta V^n(\mathbf{r}'' - \mathbf{R}_n) \int d^3r' \chi^n(\mathbf{r}'' - \mathbf{R}_n, \mathbf{r}' - \mathbf{R}_n) \times \left(\partial_{\mathbf{R}_n} \frac{Z_n}{|\mathbf{r}' - \mathbf{R}_n|} \right). \tag{23}$$

By considering the change of the nuclear potential $\partial_{\mathbf{R}_n}(-Z_n/|\mathbf{r}' - \mathbf{R}_n|)$ due to an infinitesimal shift of the nucleus as a small perturbation, the r' integral can be interpreted as the corresponding change of the on-site core charge density. This change can be easily evaluated since it gives just a rigid shift of the unperturbed and spherically symmetric core density. Therefore the r' integral is identical to

$$-\partial_{\mathbf{R}_n} \rho_c^{0n}(|\mathbf{r}'' - \mathbf{R}_n|) = \partial_{\mathbf{r}''} \rho_c^{0n}(|\mathbf{r}'' - \mathbf{R}_n|) \tag{24}$$

and thus Eq. (23) becomes

$$\mathbf{F}^n_{\mathrm{pol}} = \int d^3r \Delta V^n(\mathbf{r} - \mathbf{R}_n) \partial_{\mathbf{r}} \rho_c^{0n}(|\mathbf{r} - \mathbf{R}_n|). \tag{25}$$

Integrating by parts, we finally obtain

$$\mathbf{F}^n_{\rm pol} = -\int d^3r \rho_c^{0n}(|\mathbf{r}-\mathbf{R}_n|)\partial_{\mathbf{r}} V^n(\mathbf{r}-\mathbf{R}_n), \qquad (26)$$

where $V^n(\mathbf{r}-\mathbf{R}_n)$ is the total effective potential in cell n, including also its spherical part, which gives no contribution to the force. The total force on ion n can therefore be obtained by combining the force on the nucleus and the force on the core electrons according to Eq. (22). Denoting by $\mathbf{r}$ again site-centered coordinates we have

$$\mathbf{F}^n = Z^n \partial_{\mathbf{r}} V_C^n(\mathbf{r})|_{\mathbf{r}=0} - \int d^3r \rho_c^{0n}(r)\partial_{\mathbf{r}} V^n(\mathbf{r}), \qquad (27)$$

where V_C^n is the Coulomb part of the effective one-electron potential in cell n due to all electrons and all other nuclei outside this cell. Clearly, the first term is the force on the nucleus, evaluated with spherical core charge densities, and the second term is the force on the core electrons. Since V^n is the effective Kohn-Sham potential, the latter term includes both electrostatic and exchange-correlation contributions arising from the exchange and correlation between core and valence electrons. From Eq. (27) it is obvious that the force on the nucleus is to a large extent compensated by a nearly equal but opposite force on the core electrons. In deriving the ionic force formula (27) we have only assumed that the unperturbed core density is spherically symmetric. Therefore Eq. (27) is equally valid if one makes the frozen-core approximation[26] or if the core states are allowed to relax retaining the spherical symmetry, as it is usually done in all-electron calculations.

Using the angular momentum expansion (4) for the potential, one finally obtains for the $i=x,y,z$ component of the force on atom n

$$F_i^n = Z^n \sqrt{\frac{3}{4\pi}} \frac{V^n_{C;1i}(r)}{r}\bigg|_{r=0} - \sqrt{\frac{4\pi}{3}} \int dr \rho_c^{0n}(r) \frac{\partial}{\partial r}[r^2 V^n_{1i}(r)]. \qquad (28)$$

As we see from this result, within the KKR Green-function method the force calculation requires no additional effort since the HF force is readily calculated from the $l=1$ component of the potential and since all potential components up to $2l_{\max}$ are anyhow evaluated self-consistently.

III. TECHNICAL ASPECTS OF THE COMPUTATION

We have used our method to calculate the lattice distortion around substitutional impurities in fcc Cu. The calculations are based on the local-spin-density-functional theory[24] and employ the exchange-correlation potential of Vosko, Wilk, and Nusair.[27] An angular momentum cutoff $l_{\max}=4$ is used for the Green function, thus implying a cutoff for the potential and charge-density components at $2l_{\max}=8$. The correct shape of the WS cells is described by the proper shape functions expanded up to $4l_{\max}=16$, so that integrals over WS cells containing products of the charge density with the potential, which occur in the evaluation of the Coulomb and exchange-correlation energies, are computed exactly. The lattice constant of the Cu host, as obtained from energy minimization, is $a_0=6.7071a_B$.[15] The perturbation due to the defect was calculated self-consistently for a cluster consisting of several (5 or 12) shells of perturbed potentials around the impurity atom, while the potentials of the outer Cu atoms were assumed to be unperturbed.

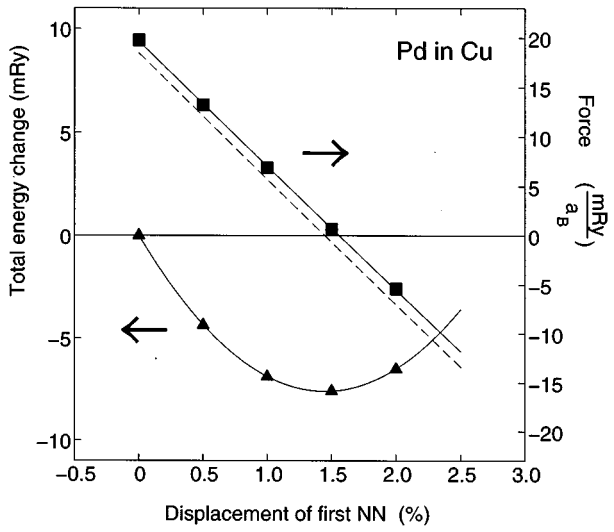

FIG. 1. Total-energy variation and radial force on a first NN atom as a function of the change of the first NN distance, for a Pd impurity in Cu. A linear fit for the force and a parabolic one for the total-energy change are shown. The force is calculated both from the HF theorem (solid line) and from the derivative of the total energy (broken line).

IV. RESULTS AND DISCUSSION

A. Are the total energy and the HF force methods consistent?

In a first approximation and in order to test our method we neglect the distortion of distant neighbors and consider only the relaxation of the first NN of the impurity, fixing all other atoms at their ideal host positions. For symmetry reasons the first NN atoms relax radially, i.e., in the $\langle 110\rangle$ directions. Their equilibrium positions can be found either from the minimum of the total energy or from the zero-force condition.

In Fig. 1 we show the change of the total energy for a Pd substitutional impurity in Cu, which was calculated including the perturbation within a cluster of 79 atoms (5 atomic shells around the impurity) for different shifts of the first NN. The total energy change shows a parabolic behavior in agreement with the harmonic approximation. Figure 1 also shows the HF force exerted on the first NN for the different radial shifts. This force is compared with the force obtained from the derivative of the total energy. The forces vary linearly with the displacement and agree well, thus demonstrating the overall consistency of our calculation. Here one should also mention that the total-energy change with displacement is very small, of the order of 1 mRy. Since 79 atoms contribute, this means that an accuracy better than 10^{-3} mRy/atom must be achieved. The use of Lloyd's formula is indispensable for that purpose. The HF force is relatively sensitive to small errors in the charge density and this sensitivity is probably the reason for the small differences between the two forces shown in Fig. 1. The parabolic behavior of the total energy with respect to the first NN dis-

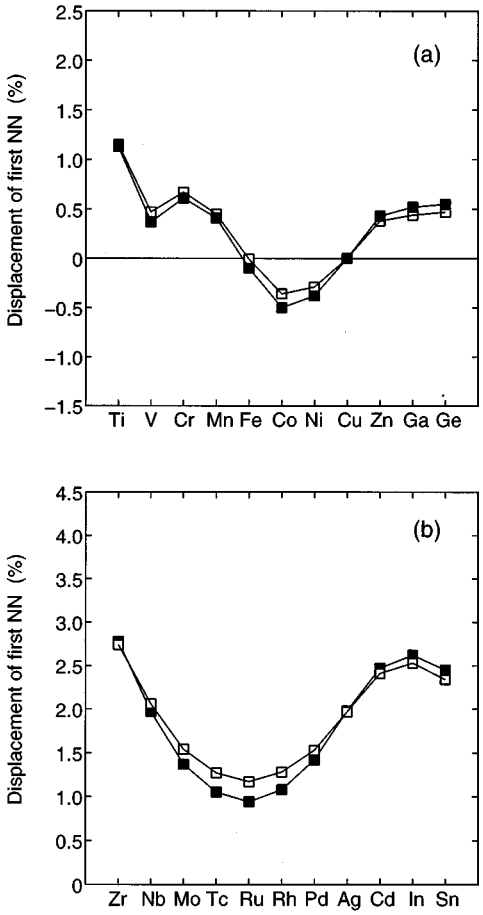

FIG. 2. Change of the first NN distance for (a) 3*d* and 4*sp* as well as (b) 4*d* and 5*sp* impurities in Cu. The results obtained from both total-energy (filled squares) and HF force (empty squares) calculations are shown.

placement and the corresponding linear variation of the force are common features for all impurities examined. The differences in the equilibrium positions predicted by the derivative of the energy and the HF force are small, as can be seen in Fig. 2, where we have plotted the first NN displacements for *d* and *sp* substitutional impurities as calculated by the above procedure, i.e., by fixing all other atoms at their ideal host positions. The differences become somewhat bigger for the 4*d* impurities and arise mainly from the difference of the forces for the unshifted positions, whereas the slopes of the force curves, i.e., the force constants, agree very well in both approaches, as can be seen from Fig. 1.

B. Treatment of the semicore states

The correct treatment of the core states is very important in order to predict the lattice distortion around impurities. One problem is connected with the fact that the core states are considered to be confined within muffin-tin (MT) spheres so that the wave function is normalized within the MT sphere. Since the MT spheres of the neighbors are centered at shifted atomic positions, they become gradually smaller with increasing lattice distortion. However, having different MT spheres for each atomic displacement leads to numerical errors arising from the different radial mesh used to solve the Schrödinger equation for the core states. Therefore, the MT radii must be sufficiently reduced so that they can be kept constant for all the considered displacements. On the other hand, reducing the radius of the MT spheres might cause problems in the calculation of the higher core (semicore) states, which can be rather extended. For Cu-based dilute alloys this problem arises only for the impurity since the Cu core states are well localized. A way to overcome this could be to treat the higher core states as valence states in a single-site approximation neglecting multiple scattering, i.e., setting the second term of the right-hand side of Eq. (1) equal to zero. In such a treatment one solves two problems. First, one gets rid of the problematic boundary conditions at the MT radius, since the Green function G_s^n is the correct solution for a single potential $V^n(\mathbf{r})$ in free space. Second, due to the full-potential treatment, the anisotropic polarization of the semicore charge density is correctly described. Thus one is not limited by the first-order perturbative approach of Sec. II C underlying the equivalence between the ionic and the original HF force formulas. Nevertheless, this approximation cannot describe the weak hybridization between semicore and valence states, which is also important for reliable force calculations. Since this requires the knowledge of the structural Green function in the energy region of the semicore states, both semicore and valence electrons must be treated on an equal footing.

TABLE I. Calculated forces on the first NN and resulting distortion around a Ti impurity in Cu using three different methods to treat the Ti 3*p* semicore state (see the text).

Case	Force (mRy/a_B)	Change of the first NN distance (%)
A	20.01	1.67
B	17.00	1.42
C	13.54	1.15

In order to demonstrate the influence of the core treatment in the force calculation we carried out three different calculations for the representative case of a Ti impurity in Cu. The results for the force exerted on the first NN at the ideal lattice position together with the resulting displacement, obtained by fixing all more distant atoms at their ideal host positions, are presented in Table I. In case *A* the semicore 3*p* states of the impurity and of the host are treated as core states with spherically symmetric core charge densities. In case *B* the Ti 3*p* state is treated as valence state, but in the single-site approximation, i.e., by neglecting the hybridization between this state and the valence states of Cu. Finally, case *C* refers to the situation where the Ti semicore state is considered as part of the valence states including the multiple scattering contributions. In case *A* the complex energy contour used to evaluate the valence charge density from Eq. (5) starts a few eV below the band minimum of Cu and ends at the Fermi energy. On the contrary, for cases *B* and *C* a very large contour starting 4.5 Ry below the Fermi level and encircling both the valence and the shallow core states is used. While the contour integral in case *A* can be accurately evaluated with about 30 complex energy points, a larger number (about 100) is needed for the large contour. Table I shows that the force on the first NN host atoms and the resulting displacement are overestimated by about 50% if the Ti 3*p* state is

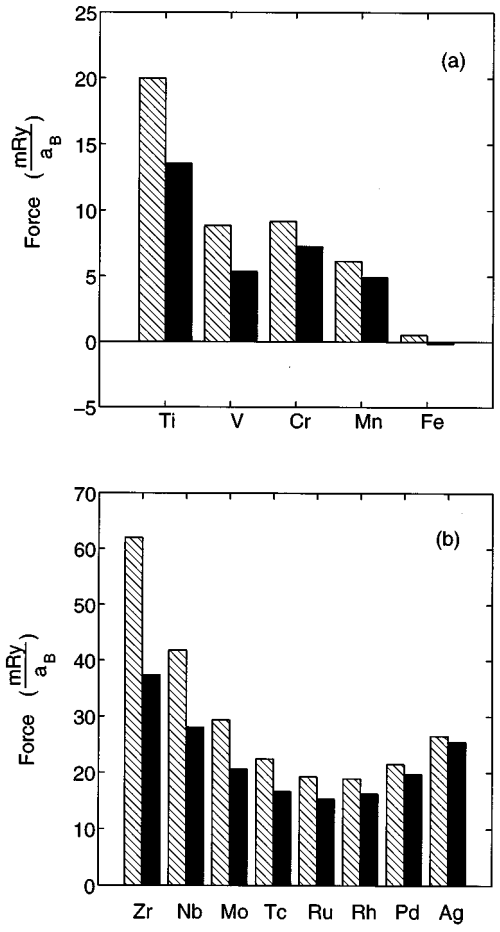

FIG. 3. Radial force on a first NN atom for (a) 3*d* and (b) 4*d* impurities in Cu, calculated using a spherical core approximation (shaded bars) and treating the shallow *p* core states of the impurities as valence states (filled bars).

considered as a core state. Even the single-site approximation (case *B*), which describes correctly the atomic polarization of the semicore state, yields too large forces.

The importance of the correct core treatment for the different impurities is demontrated in Fig. 3, where we have plotted the force exerted on the first NN around 3*d* and 4*d* impurities, calculated by both using a conventional core treatment (as described above for case *A*) and by including the shallow *p* core states in the valence band (as described for case *C*). An exception is the case of Zr, where also the lower-lying 4*s* state is included in the large complex energy contour. As can be seen, the influence of the semicore states is quite important in order to obtain the correct force. This is particularly true for the elements Ti, V, and Cr at the beginning of the 3*d* series, since the corresponding 3*p* states are more extended. This effect is even more important for the 4*d* impurities, since their 4*p* states are less localized than the 3*p* states of the isoelectronic 3*d* impurities. Due to the contraction of the semicore orbitals the effect can be neglected at the end of both series. In line with this observation we have chosen the lowest energy of the large contour 4.5 Ry below the Fermi energy, above the 3*p* state of the Cu host, thus defining an energy window within which all states are fully treated as valence states. This means that also the shallow 3*d* (4*d*) core states of the 4*sp* (5*sp*) impurities are included in this valence region. Here we should also mention that only the force on the first NN is strongly affected by the treatment of the semicore states. The forces on the more distant atoms as well as the slope of the force curve, i.e., the coupling parameters, are rather insensitive to the semicore treatment.

Figure 3 shows that the contribution to the force arising from the polarization and hybridization of the semicore states is always negative. This can be explained as follows. First of all we note that, compared to a spherical core treatment, the total energy should decrease when polarization and hybridization effects of the semicore orbitals are included. Furthermore, this decrease becomes gradually larger when the neighboring atoms come closer to the impurity because then hybridization and polarization effects become more important. This means that the error to the total energy is a decreasing function of the first NN distance, which implies an additional repulsive force when the semicore electrons are not treated correctly.

C. Lattice relaxation effects

In principle, the equilibrium position of all the atoms in the defect region can be determined by minimizing the total energy. However, this approach is rather cumbersome and needs several self-consistent calculations. On the other hand, the HF forces on all atoms can be reliably calculated from a single self-consistent calculation and thus offer a more attractive alternative to treat the lattice-distortion problem. In the case of impurities in bulk, lattice-statics simulations can be used as a guide in order to simplify the problem of predicting the equilibrium atomic positions. Determining the forces $\mathbf{F}^n$ induced by a point defect on the neighboring atoms from the *ab initio* calculation, we can get a very good estimate of the lattice distortion using the Kanzaki model.[2] A force pattern $\mathbf{F}^n$ will cause displacements $\mathbf{s}_n$. In the harmonic approximation we have $\mathbf{F}^n=\Sigma_{n'}\Phi^{nn'}\mathbf{s}_{n'}$, where Φ denotes the force-constant matrix of the defect system. In the Kanzaki model the equilibrium atomic positions around a defect can be obtained by introducing forces in the ideal crystal. The Kanzaki force

$$\mathbf{F}_K^n=\sum_{n'}\Phi_0^{nn'}\mathbf{s}_{n'}=\mathbf{F}^n-\sum_{n'}\Delta\Phi^{nn'}\mathbf{s}_{n'} \tag{29}$$

is the force that would induce the same local distortion $\mathbf{s}_{n'}$ in the host crystal as the ''direct'' force $\mathbf{F}^n$ causes in the defect system, while $\Delta\Phi=\Phi-\Phi_0$, with Φ_0 being the force-constant matrix of the host. The relaxed geometry can be now determined by minimizing the elastic energy E_{elast} of the hypothetical ideal crystal in the presence of the Kanzaki forces. In the harmonic approximation we have[2]

$$E_{\text{elast}}=\frac{1}{2}\sum_{n,n'}\mathbf{s}_n\Phi_0^{nn'}\mathbf{s}_{n'}-\sum_n\mathbf{F}_K^n\cdot\mathbf{s}_n\,. \tag{30}$$

We assume that only the force constants coupling the impurity with the first NN change. This change $\Delta\Phi$ can be found from the *ab initio* calculations, since it is given by the difference between the slopes of the force curves (see Fig. 1) for the impurity and the pure host system. The force-constant matrix Φ_0 of the Cu host can be calculated from first principles or, as done in the present study, one can use Born–von

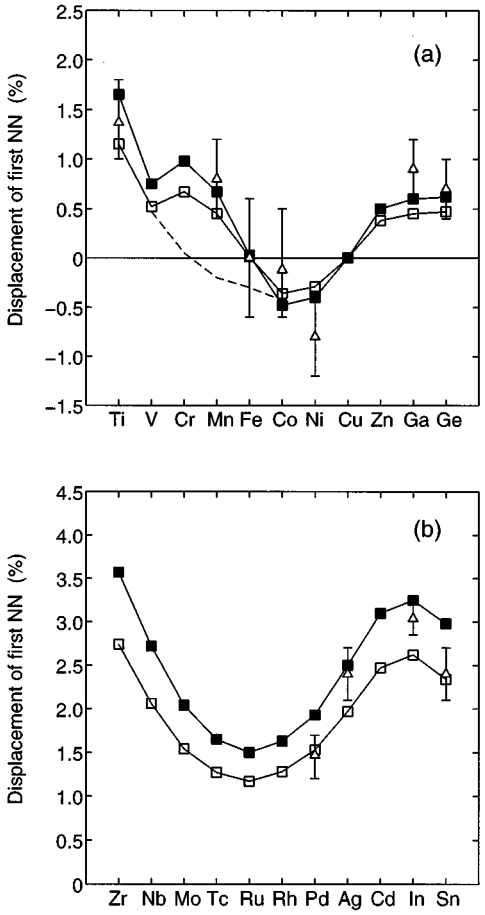

FIG. 4. Change of the first NN distance for (a) 3*d* and 4*sp* as well as (b) 4*d* and 5*sp* impurities in Cu, allowing for relaxation of one (empty squares) and all (filled squares) neighboring shells. The triangles with the error bars show the EXAFS results of Ref. 1.

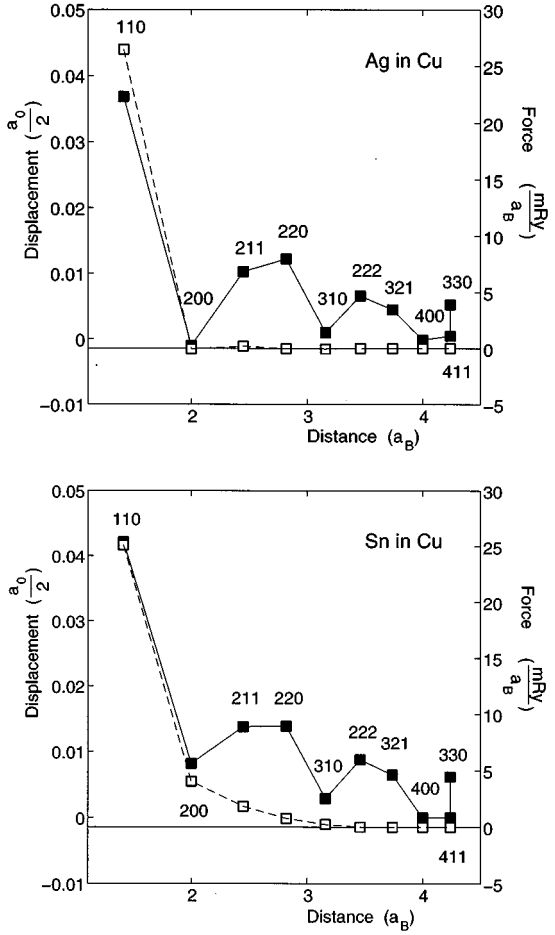

FIG. 5. HF forces (empty squares) and resulting atomic displacements (filled squares) in the neighborhood of (a) an Ag and (b) a Sn impurity in Cu.

Kármán parameters fitted to experimental phonon dispersion curves.[28] The Kanzaki forces and the corresponding atomic displacements are obtained solving Eqs. (30) and (29) self-consistently by an iterative procedure. Starting from a trial displacement for the first NN, as obtained by relaxing only the first NN (see Fig. 1), we calculate the corresponding Kanzaki forces from Eq. (29). Then, minimizing the elastic energy given by Eq. (30) with respect to $\mathbf{s}_n$, we deduce a new displacement pattern for all the atoms near the impurity. For this configuration we then recalculate the forces, etc. The iteration stops when input and output displacements are the same. We have used the relaxed atomic positions obtained from the lattice-statics simulation in a cluster of 12 shells around a Pd impurity (225 atoms) and recalculated self-consistently the forces on all these atoms in the distorted geometry. The forces were found to be rather small, less than 1 mRy/a_B.

In Fig. 4 we present the first NN relaxation obtained by using this Kanzaki procedure. For comparison we have included the approximate results shown already in Fig. 2, as calculated by fixing all other atoms at their ideal host positions. Also included are experimental data from EXAFS measurements of Scheuer and Lengeler.[1] Fixing the distant atoms at their ideal host positions results in an underestimation of the outward first NN shift. As can be seen from Fig. 4, in most cases the Cu lattice is dilated due to the substitutional defects, except for the case of Fe, Co, and Ni impurities. For a vacancy in Cu we predict a compression of the lattice with a first NN relaxation of -1.45%. In the case of 4*d* impurities the lattice distortion shows a parabolic behavior with the minimum at Ru. In contrast to this, the behavior of the 3*d* impurities is strongly influenced by magnetism. The dashed line in Fig. 4(a) indicates the results of non-spin-polarized calculations. It can be clearly seen that the magnetic 3*d* impurities experience a pronounced magnetoelastic expansion,[29] which is larger for Cr and Mn since these impurities exhibit the biggest moments in Cu. On the other hand, the influence of lattice distortion on the magnetic moments is vanishingly small. Our calculation gives for the local moments of V, Cr, Mn, Fe, and Co impurities: 0.98 (0.85), 2.96 (2.91), 3.42 (3.39), 2.53 (2.53), and 0.96 (1.01) Bohr magnetons, respectively, in the relaxed (unrelaxed) geometry. These results show that outward relaxations slightly increase the moments (V, Cr, and Mn), while inward relaxations lead to a small decrease of the magnetic moment (Co). For Fe there is no relaxation of the first NN so that, in this case, there is no moment change. This vanishingly small influence of the local lattice distortion on the impurity magnetic moment is contrary to the result obtained for, e.g., an Fe impurity in Al,[11] where the Fe magnetic moment was found to vary critically with the Al-Fe distance. This differ-

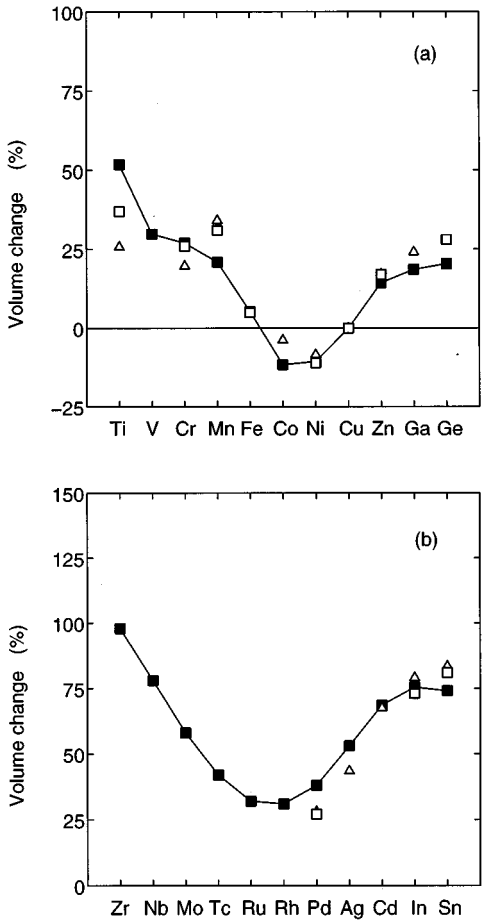

FIG. 6. Relative volume change per impurity in Cu-based dilute alloys with (a) 3*d* and 4*sp* as well as (b) 4*d* and 5*sp* impurities. The results of lattice-parameter measurements are shown with empty triangles (Ref. 32) and empty squares (Ref. 33.)

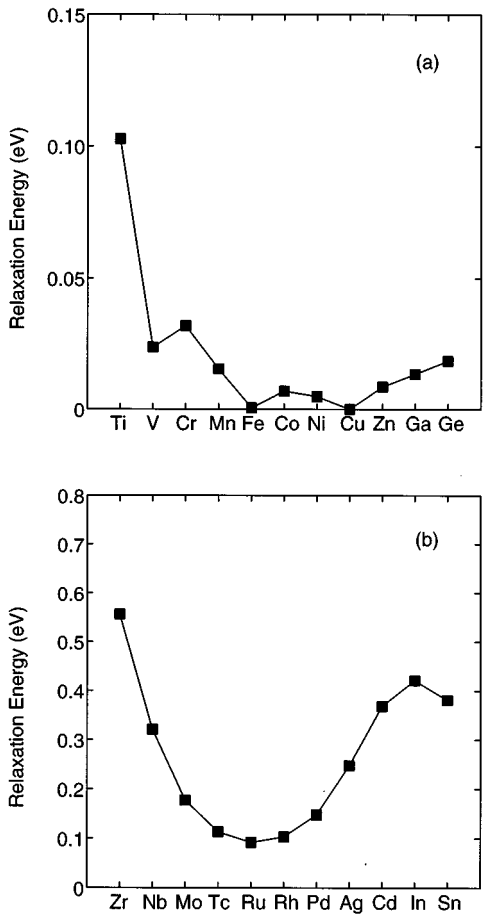

FIG. 7. Relaxation energies for (a) 3*d* and 4*sp* as well as (b) 4*d* and 5*sp* impurities in Cu.

ent behavior can be easily understood because the spin-polarization energy of the magnetic 3*d* impurities in Cu is considerably larger than the relaxation energy (see below), while the magnetic energy in the case of Fe in Al is rather small[30] and therefore lattice distortion effects can dramatically influence the magnitude of the magnetic moment.

It is interesting to take a closer look at our calculated force pattern due to the impurity atom. There is a striking difference between *d* and *sp* impurities as demonstrated in Fig. 5, where we have plotted the forces induced around an Ag and a Sn substitutional impurity in Cu, together with the resulting atomic distortion. As can be seen for Ag (similar is the behavior of all the *d* impurities), we have a strong force only on the first NN, whereas the forces on more distant neighbors vanish. This causes a displacement mainly in the $\langle 110\rangle$ directions, while we do not observe any significant distortion in the $\langle 100\rangle$ directions. On the contrary, in the case of Sn we find that also the forces on the second neighbors are appreciable, and this force pattern induces a rather isotropic distortion of the lattice at short distances. This behavior is typical for all *sp* impurities.

A lattice expansion or compression due to point defects results in a change of the host lattice constant. In the case of cubic metals the volume change due to a defect is given by the first moment of the Kanzaki forces[2]

$$\Delta V = V - V_0 = \frac{1}{3K} \sum_n \mathbf{F}_K^n \cdot \mathbf{R}^n, \tag{31}$$

where V and V_0 are the atomic volumes of the defect system and the ideal host, respectively, and K is the bulk modulus of pure Cu: $K = 1.55$ Mbar.[31] In Fig. 6 we present the calculated relative volume changes $\Delta V/V_0$ for all the systems considered in this work, together with the experimental data as obtained from lattice-parameter measurements.[32,33] For cubic crystals the volume change is related to the change of the lattice parameter by $\Delta V/V_0 = 3\Delta a/a_0$. The agreement with the experiment is good. Due to the weighting of the Kanzaki forces in Eq. (31) by $\mathbf{R}_n$ the forces on the more distant neighbors are quite important for the volume change. Since the corresponding force-constant changes are small, the use of the direct instead of the Kanzaki forces in the volume change calculation would influence the results only slightly.

We have also calculated the long-ranged lattice distortion for a single vacancy in Cu. The presence of isolated vacancies compresses the Cu lattice. We calculate a volume change of -30%, which is in very good agreement with the experimental result $(-25\pm 5)\%$.[34] It is also interesting to look at the influence of the lattice distortion on the vacancy formation energy. The relaxation energy can be calculated from $E_{\mathrm{rel}} = 1/2\Sigma_n \mathbf{F}^n \cdot \mathbf{s}_n$. We find that the vacancy formation

energy is lowered by 0.07 eV due to the lattice distortion thus obtaining a value of 1.27 eV, in perfect agreement with the experimental value of 1.28 eV.[35]

The solution energy of impurities is another important quantity influenced by lattice relaxation. In the case of 3*d* impurities the corresponding relaxation energy is quite small, typically a few hundredths of an eV. In Fig. 7 we have plotted the relaxation energy for all the systems considered in this work. It can be seen that the relaxation energy increases substantially in the beginning of the 3*d* series, since it essentially depends on the square of the displacement. The change of the elastic properties due to the defect causes only a slight reduction in the calculated distortion energies. For the 4*d* impurities we have calculated large energies, especially for the first elements of the row. However, the solubility of these impurities is quite small.

V. CONCLUSION

We have presented a method to calculate the lattice distortion around point defects in crystalline solids. The method was applied for the calculation of the equilibrium atomic positions around *d* and *sp* substitutional impurities as well as a single vacancy in Cu. Both the total energy and the HF force have been used in order to obtain the ground-state structure in the vicinity of the defect. The calculations show that within the full-potential KKR method force calculations are relatively easy, since no Pulay-type corrections (see, e.g., Ref. 36) have to be applied. They also show that for impurities in Cu reliable forces can be obtained only if the semicore states of the impurities are treated as valence states, which is particularly important for the elements at the beginning of the transition series. The atomic positions have been calculated by using lattice-statics simulations based on the Kanzaki method. The results for the shifts of the first NN and the macroscopic volume changes induced by the defect are in very good agreement with experimental data from EXAFS and lattice-parameter measurements. The present paper is an *ab initio* study of structural changes around point defects in transition metals within the framework of the KKR Green-function method. It opens the way to investigate dynamical properties of solids, structural relaxations at surfaces or around defects at surfaces where the reduced coordination number implies a greater structural flexibility.

ACKNOWLEDGMENTS

We would like to thank Dr. H. R. Schober for providing his lattice-statics code and for helpful discussions. This work was supported by a bilateral German-Greek cooperation grant. It has also benefited from collaborations within the HCM Network ''*Ab initio* (from electronic structure) calculation of complex processes in materials'' (Contract No. ERBCHRXCT 930369).

[1] U. Scheuer and B. Lengeler, Phys. Rev. B **44**, 9883 (1991).

[2] G. Leibfried and N. Breuer, *Point Defects in Metals I* (Springer-Verlag, Berlin, 1978).

[3] J. L. Martins and A. Zunger, Phys. Rev. B **30**, 6217 (1984); A.-B. Chen and A. Sher, *ibid.* **32**, 3695 (1985); W. A. Harrison and E. A. Kraut, *ibid.* **37**, 8244 (1988); F. Bechstedt and W. A. Harrison, *ibid.* **39**, 5041 (1989).

[4] R. Benedek, L. H. Yang, C. Woodward, and B. I. Min, Phys. Rev. B **45**, 2607 (1992); R. Pawellek, M. Fähnle, C. Elsässer, K. M. Ho, and C. T. Chan, J. Phys. Condens. Matter **3**, 2451 (1991); U. Breier, W. Frank, C. Elsässer, M. Fähnle, and A. Seeger, Phys. Rev. B **50**, 5928 (1994).

[5] Y. Bar-Yam and J. D. Joannopoulos, Phys. Rev. Lett. **52**, 1129 (1984); Phys. Rev. B **30**, 1844 (1984).

[6] D. J. Chadi and K. J. Chang, Phys. Rev. Lett. **60**, 2187 (1988); D. J. Chadi, *ibid.* **72**, 534 (1994); **77**, 861 (1996).

[7] J. Furthmüller and M. Fähnle, Phys. Rev. B **46**, 3839 (1992).

[8] G. A. Baraff and M. Schlüter, Phys. Rev. B **30**, 1853 (1984); Phys. Rev. Lett. **55**, 1327 (1985).

[9] M. Scheffler, J. P. Vigneron, and G. B. Bachelet, Phys. Rev. Lett. **49**, 1765 (1982); Phys. Rev. B **31**, 6541 (1985); M. Scheffler, Physica **146B**, 176 (1987).

[10] R. Car, P. J. Kelly, A. Oshiyama, and S. T. Pantelides, Phys. Rev. Lett. **52**, 1814 (1984); **54**, 360 (1985).

[11] D. Guenzburger and D. E. Ellis, Phys. Rev. Lett. **67**, 3832 (1991); Phys. Rev. B **49**, 6004 (1994).

[12] C. P. Ewels, R. O. Jones, S. Öberg, J. Miro, and P. Deak, Phys. Rev. Lett. **77**, 865 (1996).

[13] K. Jackson, M. R. Pederson, and B. M. Klein, Phys. Rev. B **43**, 2364 (1991).

[14] R. Podloucky, R. Zeller, and P. H. Dederichs, Phys. Rev. B **22**, 5777 (1980); P. J. Braspenning, R. Zeller, A. Lodder, and P. H. Dederichs, *ibid.* **29**, 703 (1984); R. Zeller, J. Phys. C **20**, 2347 (1987).

[15] R. Zeller, Int. J. Mod. Phys. C **4**, 1109 (1993).

[16] B. Drittler, Ph.D. thesis, RWTH Aachen, 1990 (unpublished).

[17] P. H. Dederichs, B. Drittler, and R. Zeller, in *Application of Multiple Scattering Theory to Materials Science*, edited by W. H. Butler, P. H. Dederichs, A. Gonis, and R. Weaver, MRS Symposia Proceedings No. 253 (Materials Research Society, Pittsburgh, 1992), p. 185.

[18] B. Drittler, M. Weinert, R. Zeller, and P.H. Dederichs, Phys. Rev. B **39**, 930 (1989).

[19] R. Zeller, J. P. Deutz, and P. H. Dederichs, Solid State Commun. **44**, 993 (1982).

[20] A. Lodder, J. Phys. F **6**, 1885 (1976).

[21] N. Stefanou, P. J. Braspenning, R. Zeller, and P. H. Dederichs, Phys. Rev. B **36**, 6372 (1987).

[22] K. Abraham, Diploma thesis, RWTH Aachen, 1991 (unpublished).

[23] N. Stefanou, H. Akai, and R. Zeller, Comput. Phys. Commun. **60**, 231 (1990); N. Stefanou and R. Zeller, J. Phys. Condens. Matter **3**, 7599 (1991).

[24] P. Hohenberg and W. Kohn, Phys. Rev. **136**, B864 (1964); W. Kohn and L. J. Sham, *ibid.* **140**, A1133 (1965).

[25] H. Hellmann, *Einführung in die Quantenchemie* (Deuticke, Leipzig, 1937); R. P. Feynman, Phys. Rev. **56**, 340 (1939).

[26] J. Harris, R. O. Jones, and J. E. Müller, J. Chem. Phys. **75** (8), 3904 (1981).

[27] S. H. Vosko, L. Wilk, and M. Nusair, J. Can. Phys. **58**, 1200 (1980).

[28] *Metals: Phonon States, Electron States and Fermi Surfaces*, edited by K.-H. Hellwege and J. L. Olsen, Landolt-Börnstein, New Series, Group III, Vol. 13, Pt. a (Springer-Verlag, Berlin, 1981), p. 1.

[29] P. H. Dederichs, T. Hoshino, B. Drittler, K. Abraham, and R. Zeller, Physica B **172**, 203 (1991).

[30] Ph. Mavropoulos, N. Papanikolaou, and N. Stefanou, J. Phys. Condens. Matter **7**, 4665 (1995).

[31] V. L. Moruzzi, J. F. Janak, and A. R. Williams, *Calculated Electronic Properties of Metals* (Pergamon, New York, 1978).

[32] H. W. King, J. Mater. Sci. **1**, 79 (1966).

[33] W. B. Pearson, *A Handbook of Lattice Spacings and Structures of Metals and Alloys* (Pergamon, London, 1958), Vol. 1, p. 570; *ibid.* (Pergamon, Oxford, 1967), Vol. 2, p. 868.

[34] P. Ehrhart, K. H. Robrock, and H. R. Schober, in *Physics of Radiation Effects in Crystals*, edited by R. A. Johnson and A. N. Orlov (Elsevier, Amsterdam, 1986), p. 3.

[35] *Atomic Defects in Metals*, edited by H. Ullmaier, Landolt-Börnstein, New Series, Group III, Vol. 25, Pt. a (Springer-Verlag, Berlin, 1991), p. 233.

[36] M. Fähnle, C. Elsässer, and H. Krimmel, Phys. Status Solidi B **191**, 9 (1995).